Nuclear Engineering and Technology 48 (2016) 1321–1329

Available online at ScienceDirect

Nuclear Engineering and Technology

journal homepage: www.elsevier.com/locate/net

Original Article

Investigation of Characteristics of Passive Heat Removal System Based on the Assembled Heat Transfer Tube

Xiangcheng Wu, Changqi Yan, Zhaoming Meng, Kailun Chen, Shaochuang Song, Zonghao Yang, and Jie Yu*

Fundamental Science on Nuclear Safety and Simulation Technology Laboratory, Harbin Engineering University, Nantong Street, Harbin 150001, Heilongjiang, China

ARTICLE INFO

Article history:
Received 28 March 2016
Received in revised form
26 June 2016
Accepted 9 August 2016
Available online 12 September 2016

Keywords:
Assembled Heat Transfer Tube
Molten Salt Reactor
Natural Circulation
Passive Heat Removal System

ABSTRACT

To get an insight into the operating characteristics of the passive residual heat removal system of molten salt reactors, a two-phase natural circulation test facility was constructed. The system consists of a boiling loop absorbing the heat from the drain tank, a condensing loop consuming the heat, and a steam drum. A steady-state experiment was carried out, in which the thimble temperature ranged from 450°C to 700°C and the system pressure was controlled at levels below 150 kPa. When reaching a steady state, the system was operated under saturated conditions. Some important parameters, including heat power, system resistance, and water level in the steam drum and water tank were investigated. The experimental results showed that the natural circulation system is feasible in removing the decay heat, even though some fluctuations may occur in the operation. The uneven temperature distribution in the water tank may be inevitable because convection occurs on the outside of the condensing tube besides boiling with decreasing the decay power. The instabilities in the natural circulation loop are sensitive to heat flux and system resistance rather than the water level in the steam drum and water tank. RELAP5 code shows reasonable results compared with experimental data.

1. Introduction

According to the International Atomic Energy Agency's definition, a passive component is a component that is self-sustained without external energy [1] and can be activated by natural laws, e.g., gravity, inertia, negative feedback. For instance, with the help of inertia, heavy flywheels on the main pump in the primary circuit in pressurized water reactors can prolong the run time of the coolant pump. The negative feedback of temperature and reactivity helps prevent the nuclear reactor core from being supercritical. These passive techniques in nuclear energy were classified by Zhou et al [2].

Of these passive techniques, the driving mechanism behind natural circulation is the density difference in the

* *Corresponding author.*
E-mail address: changqi_yan@163.com (C. Yan).
http://dx.doi.org/10.1016/j.net.2016.08.007

system loop caused by gravity. Natural circulation eliminates the possibility of pump failure. Consequently, it has been widely employed in the passive residual heat removal system (PRHRS), which usually comprises a heat exchanger, a heat source (decay heat), a heat sink, and pipelines where single- or two-phase fluid acts as a heat carrier. Park et al [3] conducted an experimental investigation into the heat transfer and natural circulation of the PRHRS for an integral type reactor called SMART (System-integrated Modular Advanced ReacTor) using a high temperature/high pressure thermal–hydraulic test facility. The operating pressure was 3.5 MPa. The results showed that their emergency cooldown tank was large enough to remove the core decay heat. Due to the complete condensation of steam in the upper part of the emergency cooldown tank, an uneven distribution of fluid temperature was recorded along the vertical direction. A PRHRS for the secondary circuit of pressurized water reactors was built and the natural circulation characteristics at the steady and transient states were studied by Wu et al [4]. The relevant experiments showed the feasibility and efficiency of the PRHRS. A Compact Integral Effects Test (CIET 1.0) was conducted at the University of California, Berkeley, CA, USA [5,6]. CIET 1.0 was scaled based on an earlier design of 900 MWh advanced high-temperature reactor. The direct reactor auxiliary cooling system in CIET 1.0 used for decay heat removal is a single-phase loop without boiling. Wang et al [7,8] planned to build a PRHRS for the molten salt reactor (MSR) based on NaK heat pipes in Xi'an Jiaotong University, Shanxi, China.

Numerical analysis of the PRHRS has been widely carried out using RELAP5 code, which was developed at the Idaho National Engineering Laboratory, Idaho Falls, USA. RELAP5 is also the basis of some other codes. For instance, the MARS code, based on RELAP5, was used for parameter study of the PRHRS in a SMART plant [9]. The effects of hydraulic resistance, valve actuation time, and initial pressure were evaluated. Nevertheless, the capability and reliability of RELAP5 has been questioned by some researchers, since numerical damping was built in RELAP5 to achieve stable solutions. Numerical damping overwhelms instabilities and renders the simulation of instabilities nonconservative [10]. Kozmenkov et al [11] validated the RELAP5 code against measurement data from natural circulation experiments performed at the CIRCUS (CIRculation Under Start-up) facility. The calculation results were in good agreement with the experimental data. The experimental results of CIET 1.0 were also used for the validation of RELAP5-3D and an excellent agreement under steady-state natural circulation was found. Mangal et al [12] found a significant difference between the numerical results and the experimental data for the parallel circulation loop. But the prediction of two-phase stable flow showed a good agreement with experimental data for the high pressure natural circulation loop. In Martin and Taylor's [13] research, some deficiencies including geometric multidimensional and form loss effects were found. There is no consensus on the capability of RELAP5 code. More validations of the PRHRS are needed.

Even though many studies have been carried out on the PRHRS in nuclear reactors, more investigations, especially experimental ones, are needed for the PRHRS of MSR with a high temperature thimble and low operation pressure. Consequently, we built a single tube natural circulation loop composed of an assembled tube, a steam drum, a heat exchanger and associated pipes. The assembled heat transfer tube was modified based on Sun et al's [14] design. The water tank is large enough for heat removal. The purpose of this work is to evaluate the feasibility of the PRHRS and study the system behavior under different operating parameters. A passive heat removal experiment was carried out. Effects of some important parameters including heat power, water level in the water tank, system resistance, and water level in the steam drum were analyzed. The capability of RELAP5 code predicting the stable flow of the PRHRS was also validated.

2. Experimental apparatus

Fig. 1 shows the assembled tube schematic of the PRHRS. The assembled tube consists of a center tube and a bayonet. Water flows downward in the center tube from the steam drum, reverses at the bottom of the bayonet, then flows up in the annulus between the bayonet and the center tube and returns to the steam drum from the top of the bayonet. Heat is input from the outer surface of the bayonet, so water boils and steam is generated in the annulus. The mixture density of water and steam in the annulus is lower than that in the center tube. Thus, the circulation in the assembled tube can be driven by density difference. For convenience, the water loop below the steam drum is called the *boiling loop*. Water and steam are separated in the steam drum by gravity. Then steam flows up and condenses in the condenser. The condensed water flows back to the steam drum due to gravity. The steam loop above the steam drum is called the *condensing loop*.

The bayonet is partially inserted into the thimble that reaches temperatures as high as hundreds of degrees Celsius. Heat in the gas gap filled with air between the bayonet and the thimble is transferred by conduction and radiation. Convection is so weak that it can be ignored. The gas gap is to increase the temperature gradient to prevent boiling crisis on the inner surface of the bayonet. A high-temperature tube furnace is used to create a high temperature on the outer surface of the thimble. Heat is transferred by radiation from the heat wire in the furnace. The heat section of the tube furnace is divided into three segments, each of which can automatically control and adjust temperature due to proportional–integral–derivative technology. The furnace is wrapped by adiabatic ceramic fiber of 250 mm in thickness, and the adiabatic layer on the outer surface of the associated pipes is 50 mm thick. Heat dissipation from the circulation loop can be ignored. The assembled heat transfer tube is a full-scale tube modified based on Sun et al's [14] design. The sufficient condenser arranged in the water tank has seven condensing tubes. To some extent the design of the condenser is arbitrary because the purpose of the condenser is to keep the natural circulation system running under a low pressure closed to the atmosphere. We hope that this experiment can give us some information about the assembled tube running at a low pressure under natural circulation with the high temperature thimble. The detailed dimensions of the system components are listed in Table 1.

When the furnace is started, the water inventory in the loop is gradually heated to saturation. As the temperature and

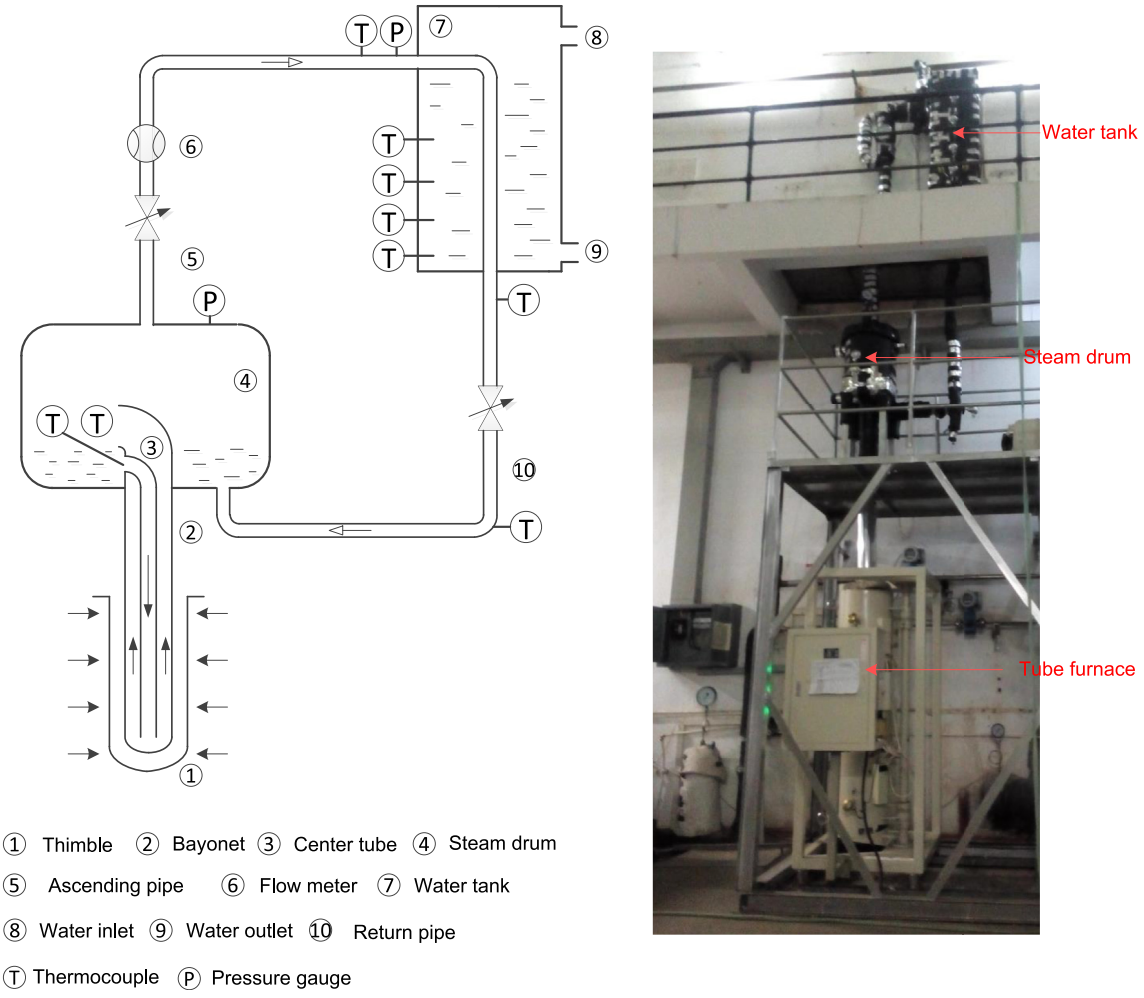

Fig. 1 – Schematic of the single tube circulation loop.

Table 1 – Dimensions of the system component.

Component	Dimension
Center tube	12.7 mm × 1.0 mm, 3 m in length
Bayonet	25.4 mm × 1.5 mm, 3.1 m in length
Thimble	38 mm × 1.5 mm, 1.5 m in length
Steam drum	300 mm in diameter 500 mm in height
Water tank	0.4 m × 0.4 m × 1.2 m; volume = 0.192 m^3
Condenser tube	7 tubes with an outside diameter of 19 mm

pressure in the steam drum become stable, the system reaches a steady state. This enables us to study the effect of heat power, system resistance, and water level in the steam drum and the water tank. The test matrix is shown in Table 2.

Nine sheathed thermocouples have been arranged in the system to measure fluid temperature with an uncertainty of 0.5°C. Four of the thermocouples with intervals of 0.25 m from the bottom of the tank are used to measure the fluid temperature in the water tank. The temperature of the bayonet was measured by six thermocouples, which are depicted in Fig. 2. There are three extra pairs of thermocouples on the outer surface of the thimble with intervals of 0.6 m. They are used for the calculation of averaged thimble temperature. The

Table 2 – Test matrix.

No.	Heat power (kW)	Water level in the steam drum (cm)	Water level in the water tank (cm)	System resistance [15]
1–2	0.78	14, 6	60	0
3–4	1.5	14, 6	60	0
5–10	1.8	10	60	1.9, 3.1, 5.1, 11.2, 14.6, 20.3
11–19	1.8	10	100, 80, 60, 50, 40, 30, 20, 15, 10	0
20	0.5–2.3	10	60	0

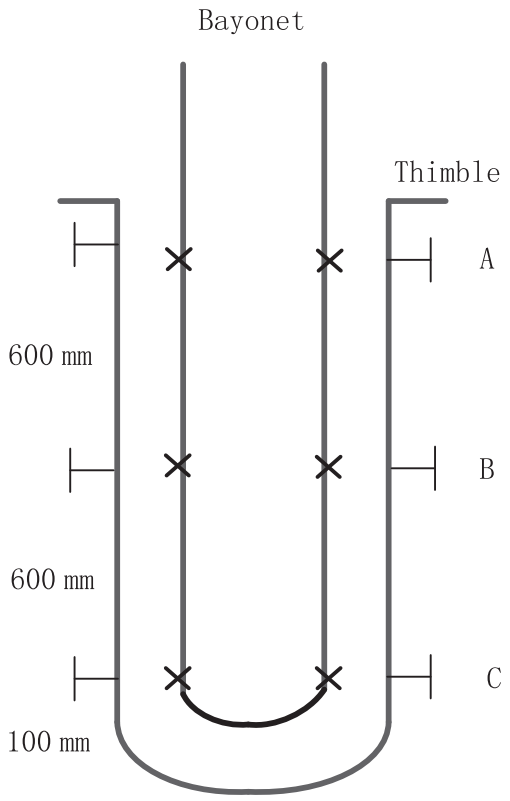

Fig. 2 – Distribution of the thermocouples.

uncertainties of these thermocouples on the thimble wall are < 4.0°C. The pressures are measured by hydrostatic pressure sensors with uncertainties of 0.04% in the full range of 0–400 kPa. Steam flow rate is measured by a rotameter with an uncertainty of 5%. Water flow rate is not measured because the center tube is fully inserted in the bayonet and the flowmeter cannot be installed in the boiling loop.

3. Results

3.1. *Effect of heat power*

As decay power decreases over time, the temperatures of the molten salt and the thimble also decline synchronously.

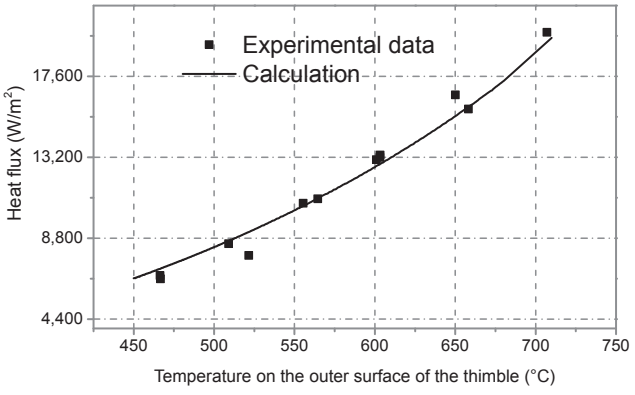

Fig. 3 – Variation of heat flux.

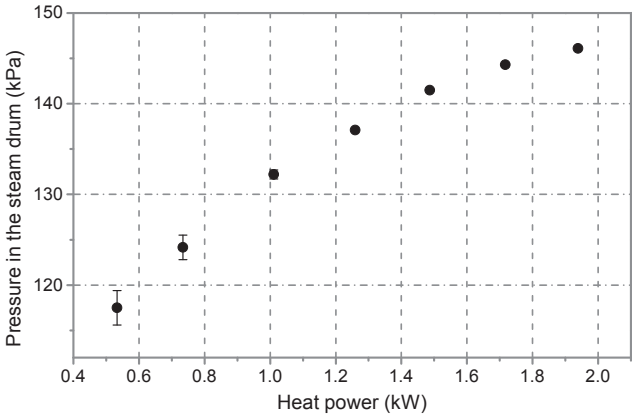

Fig. 4 – Pressure in the steam drum.

During decay heat removal, the molten salt temperature decreases from about 670°C to 480°C. The thimble temperature has a similar change. Here the thimble temperature is changed in a slightly larger change from 700°C to 450°C. Correspondingly, the heat flux also decreases, which is shown in Fig. 3.

As shown in Fig. 3, the line is calculated according to the heat transfer mechanism of radiation and conduction in the gas gap, while the points were obtained from the enthalpy difference of vapor before and after the condenser. The small deviation between the line and the points is a sign of a steady state. As the temperature increases from 450°C to 700°C, heat flux is increased by 300% from 6,500 W/m^2 to 20,000 W/m^2. For a single heat transfer tube in the drain tank, if the heat flux is lower than 6,500 W/m^2, the thimble temperature will decrease further and molten salt could be frozen. In Fig. 4, pressure fluctuates at low heat power. The error bar is used to represent the range of fluctuating. The increase in system pressure slows down as the heat power increases, which is attributed to the high compressibility of vapor. At a steady state, the system can operate below 150 kPa (slightly higher than atmospheric pressure), and all the steam is condensed into water in the condensing tube. Most of the heat released to the water tank is latent heat; only a small fraction is sensible heat. Thus most of the space at the outlet of the condenser is still filled with steam.

The wall superheat at different positions is shown in Fig. 5. The labels A–C correspond to the positions shown in Fig. 2. At low heat flux, the fluctuation of the wall superheat is relatively

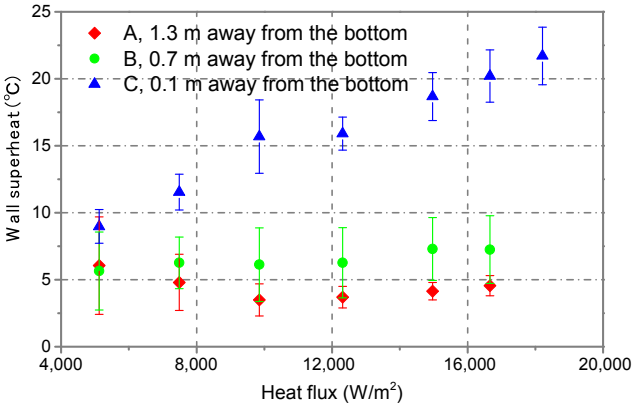

Fig. 5 – Wall superheat.

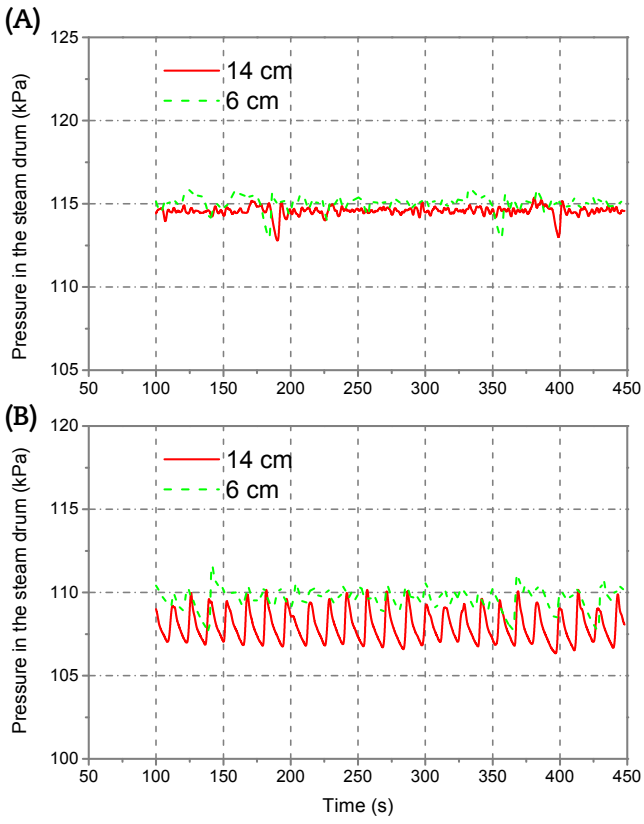

Fig. 6 – Pressures at different water levels in the steam drum. (A) 1.5 kW. (B) 0.78 kW.

large on Positions A and B, which may be attributed to intermittent boiling in the annulus. The onset of flow boiling appears on Positions A and B. As the heat flux increases, the fluctuation of wall superheat settles around a certain range. As for Position C, water is subcooled when reaching the bottom of the bayonet. Flow boiling does not occur and heat transfer is dominated by convection, so wall superheat increases with heat flux.

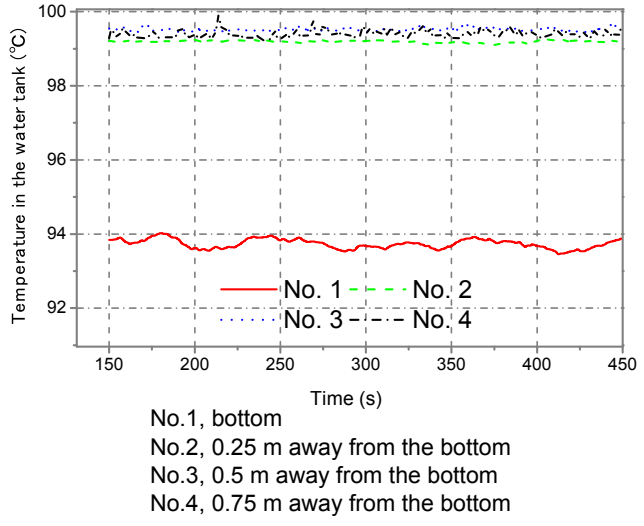

Fig. 7 – Temperature distribution in the water tank.

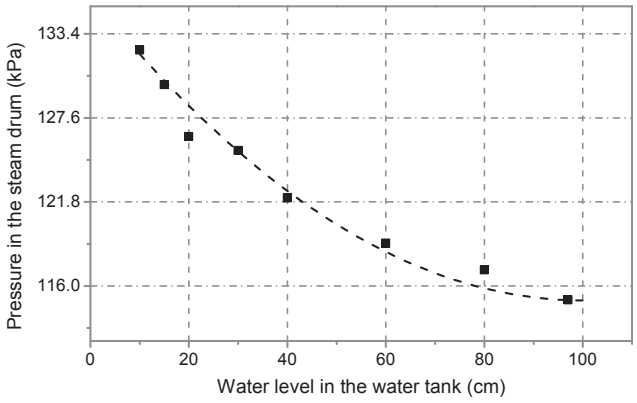

Fig. 8 – Pressures at different water levels in the water tank.

3.2. *Effect of water level in the steam drum*

The water level in the steam drum is a reflection of water inventory in the loop. The water level of the outlet of the bayonet is 12 cm. In the experiment, a low water level (6 cm) and a high water level (14 cm), which are lower and higher than the outlet of the bayonet respectively, are investigated.

Fig. 6 shows the pressures at different water levels in the steam drum. There is no notable difference of the time-averaged value between low water level (6 cm) and high water level (14 cm). The maximum amplitudes of the fluctuations are almost the same at different water levels. In theory, a high water level could slightly increase the driving force in the boiling loop, but a scaled-down test of natural circulation carried out by Basu et al [16] draws a conclusion that liquid flow rate is not influenced too much by the drum water level. Therefore, the pressure in the steam drum is insensitive to the water level.

3.3. *Effect of water level in the water tank*

The water level in the water tank decreases gradually in reality, due to evaporation and boiling. In our experiment, the water level was reduced from 100 cm to 10 cm.

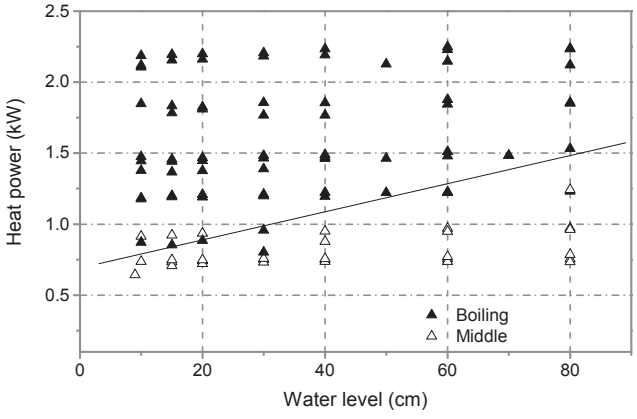

Fig. 9 – Heat transfer mode in the water tank.

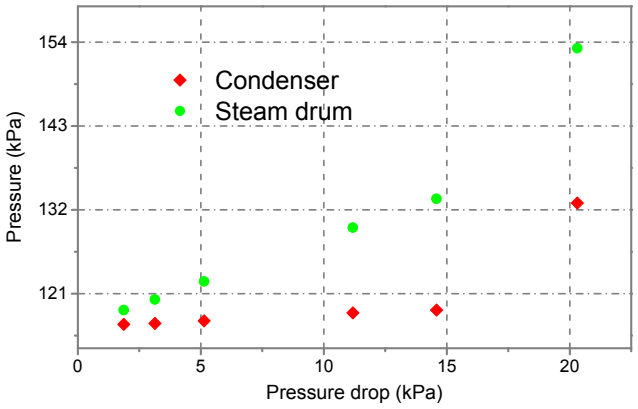

Fig. 10 – Pressures with different pressure drops.

Fig. 7 depicts the temperature distribution in the water tank along the vertical direction. Nonuniform temperature distribution can be observed. Only temperature Number 1 has a lower value; others are almost saturated. For the assembled tube, the heat capacity of the water tank is overabundant when the tank is 100% full. The system pressure is not very sensitive to the water level in the tank. As shown in Fig. 8, the pressure increases by just 14.7% when the water level in the tank decreases from 100 cm to 10 cm.

Due to relatively low velocity in the condensing tube, Reynolds number (*Re*) falls below 45. Steam is mainly condensed by film condensation in a laminar regime. The heat transfer coefficient is calculated by the analytic solution given by Nusselt. Gregorig et al [17] compared the film condensation formula [Eq. (1)] and found that it agreed well with the experimental data at low *Re*.

$$h = 0.943\left[\frac{gr\rho_l^2\lambda_l^3}{\mu_l(t_s - t_w)}\right]^{1/4} \quad (1)$$

As *Re* increases above 30, it is observed that the liquid–vapor interface becomes wavy although the flow of liquid is still laminar. The flow in this case is said to be wavy laminar. Heat transfer in a wavy laminar regime is more complicated than that in a smooth laminar regime. Kutateladze [18] suggested a modified formula for calculation of a heat transfer coefficient at $Re > 30$.

$$h_{wavy} = 0.8\mathrm{Re}^{0.11}h \quad (2)$$

From Eqs. (1) and (2), the surface temperature of the condensing tube can be obtained. To determine the heat transfer mode on the outer surface of the condensing tube, heat transfer coefficients for convection and nucleate boiling need to be calculated. Here, the formula proposed by Rohsenow [19] is used to calculate the heat transfer coefficient for pool boiling. Also heat transfer coefficient for natural circulation in an infinite space is calculated by the correlations in [20].

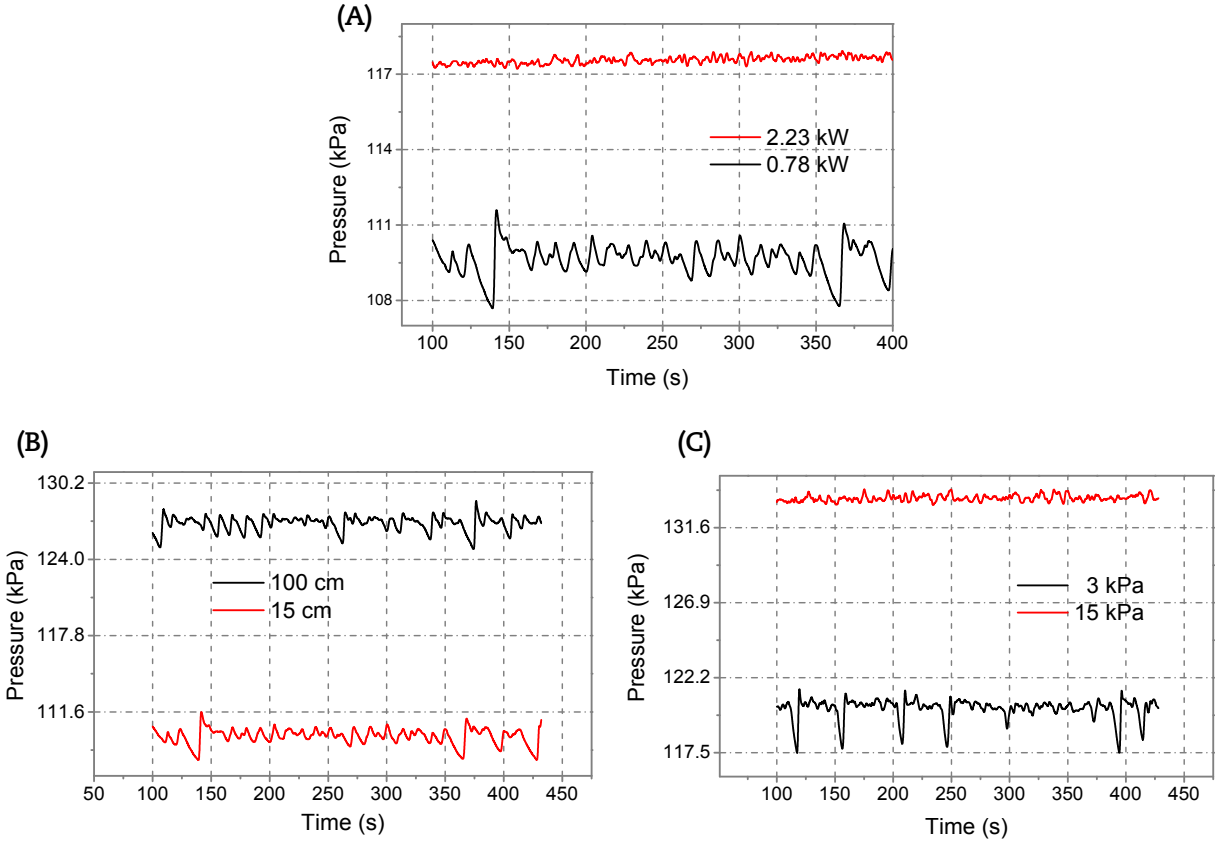

Fig. 11 – Fluctuation of pressure in the steam drum. (A) Effect of heat power. (B) Effect of water level. (C) Effect of system resistance.

The heat transfer coefficient obtained from the experimental data is compared with that obtained from convection and nucleate boiling. If the value falls between natural convection and nucleate boiling, the heat transfer mode on the outer surface of the condensing tube is marked by the label *middle*, meaning that natural convection and nucleate boiling both exist. Under other conditions, the corresponding labels *convection* and *boiling* would be used. The heat transfer modes within the experiment are shown in Fig. 9. It can be seen that most cases belong to the boiling state. The straight line gives an approximate boundary between *boiling* and *middle*. Under *middle* conditions, natural convection results in an uneven distribution of the water temperature. *Convection* conditions do not happen.

3.4. *Effect of system resistance*

On the pipes between the steam drum and the condenser in the water tank, there may be some essential instruments, like flow meters or valves, and the pressure drop may be different. So the system response to different pressure drops between the steam drum and the condenser should be investigated. In our experiment, the pressure drop is changed from 1.9 kPa to 20 kPa.

In Fig. 10, the condenser pressure increases very slightly, but a notable increase of water level in the return pipe is observed as the pressure drop is < 15 kPa. The main increase of pressure is in the steam drum. A large increase of the condenser pressure is recorded when the pressure drop is 20 kPa. This is because the water level in the return pipe goes into the condenser.

3.5. *Oscillations*

The pressure fluctuation caused by system parameters is shown in Fig. 11. As shown in Fig. 11A, pressure fluctuates greatly at low power, which is attributed to intermittent boiling/boiling delay accompanied by a sound in the bayonet. Intermittent boiling/boiling delay could also cause flow instabilities in a thermosyphon loop [21]. Chas [22] attributed

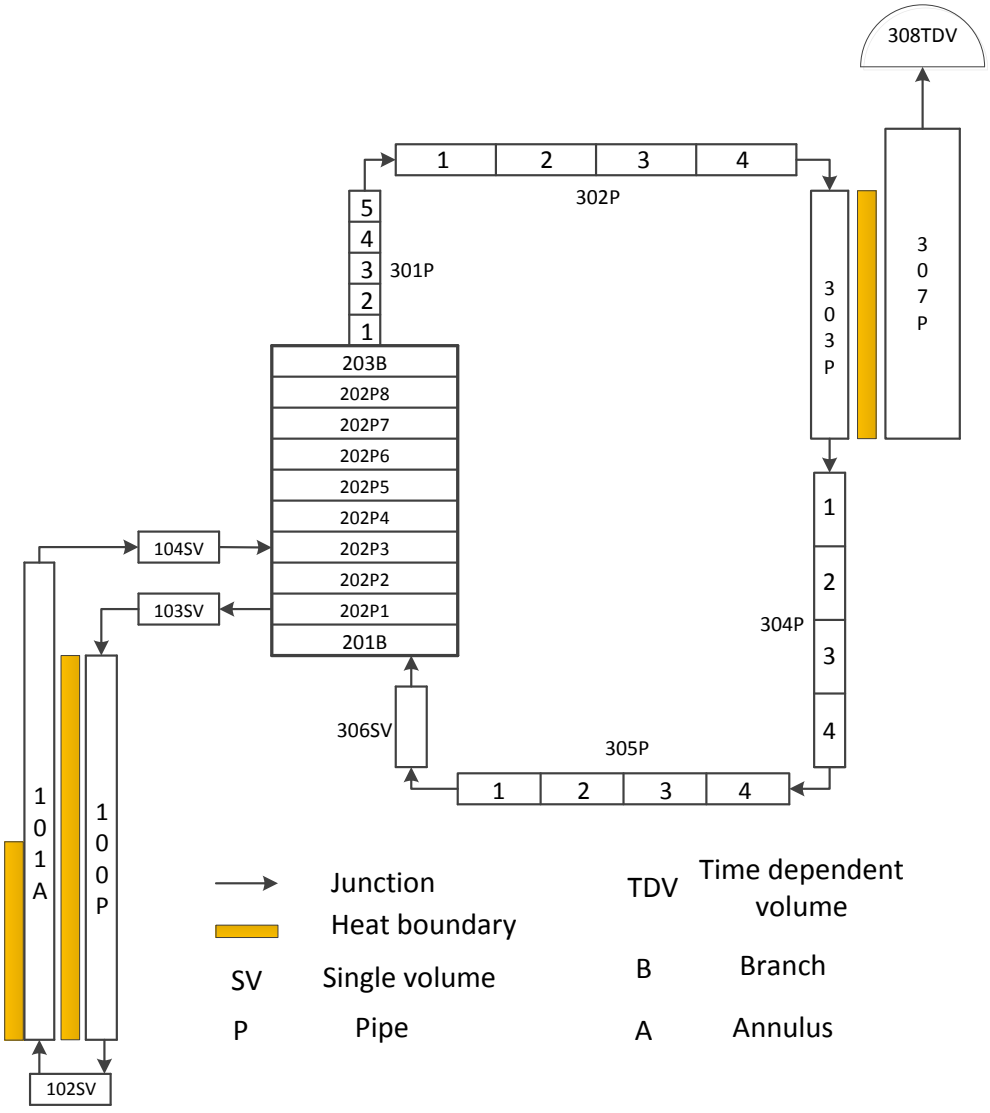

Fig. 12 – Nodalization of the system model.

intermittent boiling to the superheat of water at a certain point of contact on the tube. In our experiments, intermittent boiling disappears when heat power increases to 18.5 kW/m^2.

From the comparison in Fig. 11, the system stability is mainly influenced by heat power and system resistance instead of water level. Low system resistance and heat power have a negative effect on the stability of the system. It should be noted that density wavy oscillation could appear under some conditions with low heat power and high water level in the steam drum (Fig. 6B).

4. Validation of numerical model

4.1. *Numerical model*

A system model has been developed for the validation of the RELAP5 code. During the calculation, some simplifications are made in the two phasic continuity equations, momentum equations, and energy equations: the Reynolds stresses and Reynolds heat flux are neglected; the covariance terms are universally neglected (unity assumed for covariance multipliers); the interfacial momentum storage and energy storage are neglected; and finally the phasic viscous stresses and internal phasic heat transfer are neglected.

In RELAP5, the hydraulic components, their connections, and the heat structures in contact with fluid are modeled by volumes (also known as nodes), junctions, and heat structure modules, respectively. The system model is shown in Fig. 12. Single volume means a component that has only one volume. Pipe and annulus can have more than one volume. Branch usually has two or more junctions. Time dependent Volume can give boundary conditions. 100P simulates the downward channel in the center tube, and 101A simulates the annulus between the center tube and the bayonet. There are 30 and 31 nodes in 100P and 101A, respectively. Each node of 100P and 101A represents a distance of 0.1 m in the axial direction. 201B, 202P, and 203B simulate the steam drum. The condenser is modeled by 303P with 10 volumes and the water tank is modeled by 307P with 12 volumes. The associated pipes between the steam drum and the condenser are simulated by 301P, 302P, 304P, 305P, and 306SV.

A constant atmosphere pressure is given by 308TDV. Heat transfer is modeled by the heat boundary between 303P and 307P. Heat transfer between the annulus and the downward channel is modeled by the heat boundary between 100P and 101A. The heat boundary on the left side of 101A is specified by heat flux obtained in the experiment. Other components are considered adiabatic.

In the system model, Chen's [23] formula is used to calculate the heat transfer coefficient before critical heat flux. The default option of film-wise condensation is the maximum of the Nusselt (laminar) and Shah (turbulent). Mangal et al [12] presented the hydrodynamic models in detail.

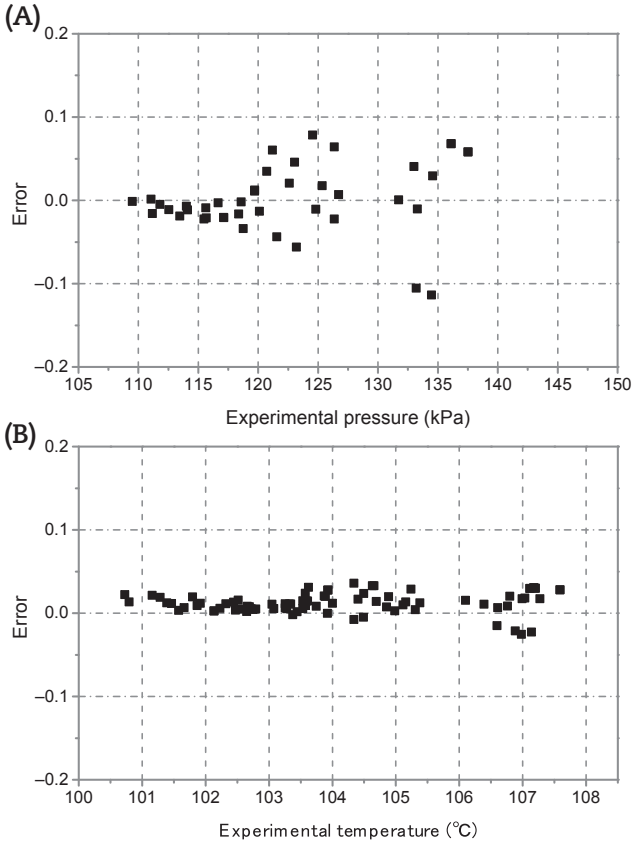

Fig. 13 – Validation of the system model. (A) Pressure. (B) temperature.

4.2. *Validation*

Fig. 13 shows the deviation between calculated values and experimental data. The experimental pressures and temperatures are obtained in the steam drum. The error is defined in the following:

$$Error = \frac{Calculated\_data - Experimental\_data}{Experimental\_data} \quad (3)$$

The maximum pressure error is 11% at 0.78 kW with water level of 10 cm in the water tank. Most of the pressure points fall within ± 8% and the temperature errors are within ± 5%. The large error at high pressures may be attributed to the deviation of boiling models. From the above discussion, boiling and convection both exist on the outer surface of the condensing tubes. As the pressure increases, the boiling mechanism becomes dominant and the deviation becomes large.

5. Conclusions

A natural circulation experiment simulating the PRHRS of MSR based on an assembled tube was carried out and the corresponding system model was validated. Some main conclusions are summarized as follows. (1) The natural circulation system is feasible in removing the decay heat even though some fluctuations such as intermittent boiling may occur in the operation. An uneven distribution of fluid temperature in the water tank was observed at high water levels. Moreover, the uneven temperature distribution may be inevitable because convection occurs on the outside of the condensing tube besides boiling when the decay power

decreases. (2) Intermittent boiling and density wave oscillation may occur at low heat flux, but the instabilities did not show a severe impact on system operation due to their small amplitudes. These fluctuations are sensitive to heat flux and system resistance rather than water level in the steam drum and water tank. It should be noted that system resistance mainly affects the steam drum pressure rather than the condenser pressure. The system model shows reasonable results compared with the experimental data.

Conflicts of interest

All authors have no conflicts of interest to declare.

Acknowledgments

This work is supported by the National Natural Science Foundation of China under Grant No. 11475048.

Nomenclature

h	Heat transfer coefficient (W/m^{2}s)
ρ	Density (kg/m^3)
λ	Heat conductivity (W/ms)
r	Latten heat (J/kg)
t	Temperature (°C)
Re	Reynolds number

Subscripts

l	liquid
s	saturated
w	wall

REFERENCES

[1] M.H. Prasad, A.J. Gaikwad, A. Srividya, A.K. Verma, Failure probability evaluation of passive system using fuzzy Monte Carlo simulation, Nucl. Eng. Design 241 (2011) 1864–1872.
[2] T. Zhou, J. Li, X. Ru, C. Sheng, J. Chen, Y. Huang, Z. Xiao, Application and development of passive technology in nuclear power units, Proc CSEE 33 (2013) 81–89.
[3] H.S. Park, K.Y. Choi, S. Cho, C.K. Park, S.J. Yi, C.H. Song, M.K. Chung, Experiments on the heat transfer and natural circulation characteristics of the passive residual heat removal system for an advanced integral type reactor, J. Nucl. Sci. Technol. 44 (2007) 703–713.
[4] J. Wu, Q. Bi, C. Zhou, Experimental study on circulation characteristics of secondary passive heat removal system for Chinese pressurized water reactor, Appl. Thermal Eng. 77 (2015) 106–112.
[5] P. Bardet, E. Blandford, M. Fratoni, A. Niquille, E. Greenspan, P.F. Peterson, Design, analysis and development of the modular PB-AHTR, American Nuclear Society, La Grange Park (IL), 2008.
[6] J. Serp, M. Allibert, O. Beneš, S. Delpech, O. Feynberg, V. Ghetta, D. Heuer, D. Holcomb, V. Ignatiev, J.L. Kloosterman, L. Luzzi, E. Merle-Lucotte, J. Uhlíř, R. Yoshioka, D. Zhimin, The molten salt reactor (MSR) in generation IV: overview and perspectives, Prog. Nucl. Energy 77 (2014) 308–319.
[7] C. Wang, D. Zhang, S. Qiu, W. Tian, Y. Wu, G. Su, Study on the characteristics of the sodium heat pipe in passive residual heat removal system of molten salt reactor, Nucl. Eng. Design 265 (2013) 691–700.
[8] C. Wang, Z. Guo, D. Zhang, S. Qiu, W. Tian, Y. Wu, G. Su, Transient behavior of the sodium-potassium alloy heat pipe in passive residual heat removal system of molten salt reactor, Prog. Nucl. Energy 68 (2013) 142–152.
[9] Y.J. Chung, S.H. Yang, H.C. Kim, S.Q. Zee, Thermal hydraulic calculation in a passive residual heat removal system of the SMART-P plant for forced and natural convection conditions, Nucl. Eng. Design 232 (2004) 277–288.
[10] J. Paniagua, U.S. Rohatgi, V. Prasad, Modeling of thermal hydraulic instabilities in single heated channel loop during startup transients, Nucl. Eng. Design 193 (1999) 207–226.
[11] Y. Kozmenkov, U. Rohde, A. Manera, Validation of the RELAP5 code for the modeling of flashing-induced instabilities under natural-circulation conditions using experimental data from the CIRCUS test facility, Nucl. Eng. Design 243 (2012) 168–175.
[12] A. Mangal, V. Jain, A.K. Nayak, Capability of the RELAP5 code to simulate natural circulation behavior in test facilities, Prog. Nucl. Energy 61 (2012) 1–16.
[13] R.P. Martin, B.K. Taylor, Benchmarking assessment of RELAP5/MOD3 for the low flow and natural circulation experiment, Westinghouse Savannah River Co., Aiken (SC), 1992.
[14] L. Sun, L. Sun, C. Yan, D. Fa, N. Wang, Conceptual design and analysis of a passive residual heat removal system for a 10 MW molten salt reactor experiment, Prog. Nucl. Energy 70 (2014) 149–158.
[15] K.A. Dittko, M.P. Kirkpatrick, S.W. Armfield, Large eddy simulation of complex sidearms subject to solar radiation and surface cooling, Water Res. 47 (2013) 4918–4927.
[16] D.N. Basu, N.D. Patil, S. Bhattacharyya, P.K. Das, Hydrodynamics of a natural circulation loop in a scaled-down steam drum-riser-downcomer assembly, Nucl. Eng. Design 265 (2013) 411–423.
[17] R. Gregorig, J. Kern, K. Turek, Improved correlation of film condensation data based on a more rigorous application of similarity parameters, Wärme Stoffübertragung 7 (1974) 1–13.
[18] S.S. Kutateladze, Fundamentals of heat transfer, Academic Press, New York, 1963.
[19] W.M. Rohsenow, J.P. Hartnett, E.N. Ganic. Boiling, handbook of heat transfer fundamentals, McGraw-Hill, New York, 1985.
[20] Z. Tao, W. Zenghui, Y. Ruichang, Study on model of onset of nucleate boiling in natural circulation with subcooled boiling using unascertained mathematics, Nucl. Eng. Design 235 (2005) 2275–2280.
[21] R. Khodabandeh, R. Furberg, Instability, heat transfer and flow regime in a two-phase flow thermosyphon loop at different diameter evaporator channel, Appl. Thermal Eng. 30 (2010) 1107–1114.
[22] R.D. Chas, Demonstration on intermittent pressure with boiling water, Proc. Phys. Soc. London 35 (1922) 273.
[23] J.C. Chen, Correlation for boiling heat transfer to saturated fluids in convective flow, Ind. Eng. Chem. Proc. Design Devel. 5 (1966) 322–329.